CHAPTER (3)

MICROFACIES AND DIAGENESIS

CHAPTER (3)

MICROFACIES AND DIAGENESIS

3.1 Introduction

The present chapter deals with the detailed petrographic descriptions of the Cretaceous core successions from the Western Desert. The cores in the study area made up mainly of siltstones, silty fine sandstones and carbonates. Forty eight thin sections were prepared for the representative samples which were collected from the different rock units. The micro constituents of these rocks have been examined and described in detail under the polarized microscope. The petrographic study carried out in this work aims to emphasize and demonstrate the different types of lithofacies in each lithostratigraphic unit, based on the type and amount of skeletal and non skeletal particles, textures and the cementing material. According to petrographic studies the rocks are classified to non-clastic and clastic, in the present work the non-clastic rocks comprising marl and the clastic rocks comprising sandstones. The microscopic examination of the clastic and non-clastic rocks greatly helps in interpreting their depositional environment and the paleoecologic conditions as well as the diagenetic processes. It may help also in establishing a basis of correlation by means of characteristic microfacies associations. In the present study, the carbonate microfacies are described and differentiated using the classification of Dunham (1962) with modification of Embry and Klovan (1972), also the description and nomenclatures given here for the carbonate microfacies are guided with the checklists and the standard microfacies types of Wilson (1975) and Flügel (1982). With respect to the sandstones, they were described and subdivided following the classification of Pettijohn et al., (1973). Figures (3.1)-(3.6) display the stratigraphic columns of wells

BED1-11, TSW-7, TSW-8, TSW-13, TSW-15 and TSW-21 respectively. The zones of light turquoise colour in the stratigraphic columns indicate the unplugged intervals. Table (3.1) displays the abbreviations that have been used in the lithological description.

Table (3.1): Abbreviations used in the lithological description.

Rock Type		**Miscellaneous**	
Sst	Sandstone	a.a.	as above
Sltst	Siltstone	arg	argillaceous
Marl	Marl	calc	calcareous
Colour		carb	carbonaceous
brnsh	brownish	fla	flasers
gry	grey	ferr	ferruginous
dk	dark	glauc	glauconite
lt	light	hi	high
Grain Size		lam	laminated
gr	grain	mass	massive
f	fine	phos	phosphate
m	medium	pyr	pyrite
v	very	rip	ripples
Sorting		slily	slightly
srt	sorted	slty	silty
wl	well	sdy	sandy
Texture		styl	stylolite
hd	hard		

Age	Fm.	S#	Depth, m	Lithology	Description
Lower Cenomanian	L. Part of The Bahariya	2	3512.75		Sst, gry, vf gr, hd, wl srt, pyr, styl
			3513.00		
		3	3513.50		a.a
		4	3513.75		a.a., fla
			3514.00		
		5	3514.50		a.a., hi pyr, carb
		6	3514.75		a.a
		7	3515.00		a.a., ferr
		8	3515.25		a.a., glauc
		9	3515.50		a.a
			3515.75		
		12,13	3517.00		a.a., mass
		14	3517.25		a.a
			3517.50		
		15,16	3518.00		a.a
		21	3518.25		a.a
			3519.50		
		24	3519.75		a.a., rip
			3520.00		
		25	3520.75		Sst, gry, vf gr., wl srt, hd, pyr, styl
			3521.00		
		27	3521.25		a.a., rip and fla
		28	3521.50		a.a
		29	3521.75		a.a., no rip, no fla, mass
			3522.00		
		30	3522.25		Sst, gry, f gr., hd, wl srt, mass
		31	3522.50		Sst, gry, vf gr, hd, arg, ferr, pyr, carb
			3522.75		
		39	3525.25		Sst, gry, vf gr., hd, fla, arg, carb
			3525.50		
		40	3526.00		Sst, gry, vf gr, hd, rip, fla, arg,
		41	3526.25		Sst, gry, vf gr, hd, pyr, mass
			3526.50		
		43	3527.25		a.a
			3527.50		
		44	3528.00		a.a
		46	3528.25		Sst, gry, vf gr., m hd, wl srt, pyr
		47	3528.50		a.a., rip, arg, carb, styl
			3528.75		
		48	3529.00		Sst, gry, vf gr, hd, wl srt, pyr, mass
		50	3529.25		Sltst, gry, arg, m hd, pyr, mass
			3529.50		
		51	3529.75		Sst, gry, vf gr, hd, wl srt, pyr, mass
		52	3530.00		a.a., arg, fla
		53	3530.25		a.a., carb
			3530.50		
		54	3531.00		a.a
			3531.25		
		56	3531.50		Sst, gry, vf gr, hd, wl srt, fla and styl
			3531.75		
		59	3532.75		a.a
		60	3533.00		a.a., carb
			3533.25		
		62	3533.50		Sst, gry, vf gr, hd, wl srt, mass
			3533.75		
		63	3534.75		a.a
			3535.00		
		64	3536.25		a.a
			3536.50		
		65	3536.75		Sst, gry, vf gr, hd, wl srt, mass
			3537.00		
		73	3543.75		Sst, gry, vf gr, hd, glauc, pyr, fla
			3544.00		
		74.75	3544.50		a.a., rip lam, bioturbation
			3544.75		
		76	3545.50		a.a
			3545.75		
		78	3546.25		a.a., carb
		79	3546.50		Sst, gry, vf gr, hd, carb, pyr, fla lam

Legend: Sandstone, bioturbation, Siltstone, Ripples

Fig. (3.1): Stratigraphic column of BED1-11 well

Age	Fm.	S#	Depth, m	Lithology	Description
Lower Cenomanian	U. Part of The Bahariya	32	2021		Sst, gry, vf gr, hd, mass, hi arg, ferr.
			2021.9		
		10	2022.8		Sst, gry, vf gr, hd, mass, pyr.
		22H	2023.7		a.a., slily calc.
			2024.7		
		42	2026.4		a.a., ferr.
		2H2	2027.3		Sst, brnsh gry, vf gr, hd, lam, pyr, slily arg, slty, rip.
		31H1	2028.2		Sst, gry, vf gr, hd, slty, arg,rip.
		31H2	2028.6		a.a.
			2029.1		
		35	2030		a.a.
		19	2030.9		a.a.
			2031.8		
		40	2035.4		Sst, gry, hd, mass, calc, pyr, hi arg, ferr.
			2036.3		
		1H1	2037.2		Sst, gry, hd, arg.
		1H2	2037.6 2038.1		a.a.

Legend: Sandstone Ripples

Fig. (3.2): Stratigraphic column of TSW-7 well

Age	Fm.	S#	Depth, m	Lithology	Description
Upper Cenomanian	Abu Roash 'F'	57	1799.6		Marl, gry, hd, sdy, phos, carb.
		58	1799.8		a.a.
		59H2	1800		a.a.
		36	1801		a.a.
		38	1802		a.a.
		50H1	1803		a.a., pyr.
		33	1804		a.a., non pyr.
		41H1	1805		a.a.
		44	1806		a.a.
		12H1	1807		a.a.
		51	1808		a.a.
			1809		

Legend: Marl

Fig. (3.3): Stratigraphic column of TSW-8 well

Age	Fm.	S#	Depth, m	Lithology	Description
Lower Cenomanian	U. Part of The Bahariya	39	2049		Sst, brnsh gry, vf gr, hd, rip, fla, carb, pyr.
			2050		
		34	2052		a.a.
			2053		
		48H1	2055		a.a.
		48H2	2055.5		Sst, brnsh gry, vf gr, hd, rip, fla, carb, pyr.
			2056		

Legend: Sandstone Ripples

Fig. (3.4): Stratigraphic column of TSW-13 well

Age	Fm.	S#	Depth, m	Lithology	Description
Lower Cenomanian	U. Part of The Bahariya	3	2006		Sst, gry, vf gr, hd, mass, slily arg, pyr, slily calc.
		28H1	2006.5		a.a., non calc.
		28H2	2007		a.a.
			2007.5		
		13H1	2010.5		Sst, dk gry, vf gr, hd, carb, phos, pyr, mass.
		13H2	2011		a.a.
			2011.5		
		6	2013.5		Sst, gry, vf gr, hd, glauc, pyr, rip.
		55	2014.5		a.a., mass.
			2015.5		
		53H1	2072		a.a.
		53H2	2072.5		a.a.
		18H1	2073		Sst, gry, vf gr , hd, mass, pyr.
		18H2	2073.5		a.a.
		43H1	2074		Sst, gry, vf gr, hd, pyr, rip.
		43H2	2074.5		a.a.
		21H1	2075		a.a.
			2076		
		11H1	2077		Sst, gry, vf gr, hd, pyr, mass.
		11H2	2077.5		a.a.
		7H1	2078		Sst, gry, vf gr, hd, pyr, fla.
		7H2	2078.5 2079		a.a.

Legend: Sandstone Ripples

Fig. (3.5): Stratigraphic column of TSW-15 well

Age	Fm.	S#	Depth, m	Lithology	Description
Upper Cenomanian	Abu Roash `G`	17	1986.5		Sst, gry, vf gr, hd, rip, pyr, slily arg.
		25H1	1987.5		a.a.
		25H2	1988		a.a.
		30H1	1988.5		a.a.
		30H2	1989		a.a.
			1989.5		
		9H1	1990.5		Sst, gry, vf gr, slty, arg, pyr, mass, ferr.
		9H2	1991		a.a.
		24	1991.5		Sst, lt gry, vf gr, hd, mass, slily rip, pyr.
		54	1992.5		*Marl, gry, hd, sdy, pyr.*
		52	1993.5		Sst, gry, vf gr, hd, pyr, rip, fla.
			1994.5		
		16H1	1995.5		a.a.
		16H2	1996		a.a.
			1996.5		
		20H1	1998.5		a.a.
		20H2	1999		a.a.
			1999.5		
Lower Cenomanian	U. Part of The Bahariya	45	2051		Sst, gry, vf gr, hd, mass, pyr.
		5	2052		a.a., slily arg and calc.
		49	2053		Sst, gry, vf gr, hd, carb, arg, pyr, fla, slily calc.
		37	2054 2055		a.a.

Legend: Sandstone, Marl, Ripples

Fig. (3.6): Stratigraphic column of TSW-21 well

3.2 Carbonate group

3.2.1 Introduction

Biological and biochemical processes are dominant in the formation of carbonate sediments; with a few notable exceptions inorganic precipitation of CaCO3 from seawater can rarely be demonstrated. Once deposited, the chemical and physical processes of diagenesis can considerably modify the carbonate sediments. Carbonates occur throughout the world in every geological period from Cambrian onwards, and reflect the changing through evolution and extinction of invertebrates with carbonate skeletons. In Precambrian, the carbonates are often dolomitic, and many contain algal stromatolites, produced largely by the blue-green algae. The economic importance of carbonates today lies chiefly in their reservoir properties since many of the world's major petroleum reserves are contained within carbonate rocks (Chilingar et al., 1972). In our study the carbonates are represented by only one microfacies type as follows:

3.2.2 Foraminiferal molluscan packstone, (Plate 3.1, Figs. A-B)

This lithofacies is recorded in Abu Roash `F` Member in TSW-8 well (Plate 3.1, Fig. A) and Abu Roash `G` Member in TSW-21 well (Plate 3.1, Fig. B). This lithfacies is hard marly and pyritic in nature. The ground mass is composed mainly of micrite and sparry calcite, fossils as foraminiferal tests and shell fragments comprised the allochemes, some quartz grains are disseminated in the ground mass, carbonate present, no visible porosity, quartz grains are monocrystalline. This lithofacies is interpreted as offshore facies.

3.3 Sandstone group

Terrigenous clastic sediments are a diverse group of rocks, ranging from the fine-grained mudrocks, through the coarser grained sandstones to conglomerates and breccias. The sediments are largely composed of fragments or clasts, derived from pre-existing igneous, metamorphic and sedimentary rocks. The clastic grains are released through mechanical and chemical weathering processes, and then transported to the depositional site. Mechanisms involved in the transportation include the wind, glaciers, river currents, waves, tidal currents and turbidity currents. The detrital grains may be rock fragments but the majority are individual crystals, chiefly of quartz and feldspar, abraded to various degrees. The finer breakdown products of the original rocks formed during weathering and consisting mainly of clay minerals, are predominant in mudrocks and form the matrix to some sandstones and conglomerates. In a broad sense, the composition of clastic sediments is a reflection of the weathering processes, largely determined by the climate and geology of the source area. Two important features of siliciclastic sediments are the sedimentary structure and texture. Many of these are produced by the depositional processes, while others are post-depositional or diagenetic in origin.

3.4 Classification of sandstones

Numerous classifications of terrigenous clastics have been proposed over the years with the majority based on two parameters: mineralogy and/or texture. Most classifications use a triangular diagram with end members of quartz, feldspar and rock fragments. The triangle is divided into various fields, and rocks with a modal analysis falling within a particular field are given a particular name. An accepted and widely-used classification is that presented by Pettijohn et al., 1973, (Fig. 3.7) and based on Dott (1964). Sandstones are divided into two major groups based on texture that is whether the sandstones

composed of grains only (arenites) or contain more than 15% matrix, forming the wackes. Of the arenites, the term quartz arenite is applied to those with 95% or more quartz grains, a rock-type formerly referred to as quartzite or orthoquartzite. Arkosic arenite refers to an arenite with more than 25% feldspar, which exceeds the rock fragments content, and lirharenite is applied where the rock fragments content exceeds 25% and is greater than feldspar. The arkosic arenites can be divided into arkoses and lithic arkoses. Two rock-types transitional with quartz arenite are subarkose and sublitharenite. Specific names which have been applied to litharenite are phyllarenite where the rock fragments are chiefly of shale or slate, and calclithite where the rock fragments are of limestone. The wackes are the transitional group between arenites and mudrocks. The most familiar is the grey wacke and two types are distinguished: feldspathic and lithic greywacke. The term arkosic wacke is used for arkoses with a significant proportion of matrix. Quartz wackes, not a common rock-type, are dominant quartz plus some matrix. This classification is primarily concerned with the mineralogy of the sediment and presence or absence of a matrix. It is independent of the depositional environment, although some lithologies are more common in certain environments.

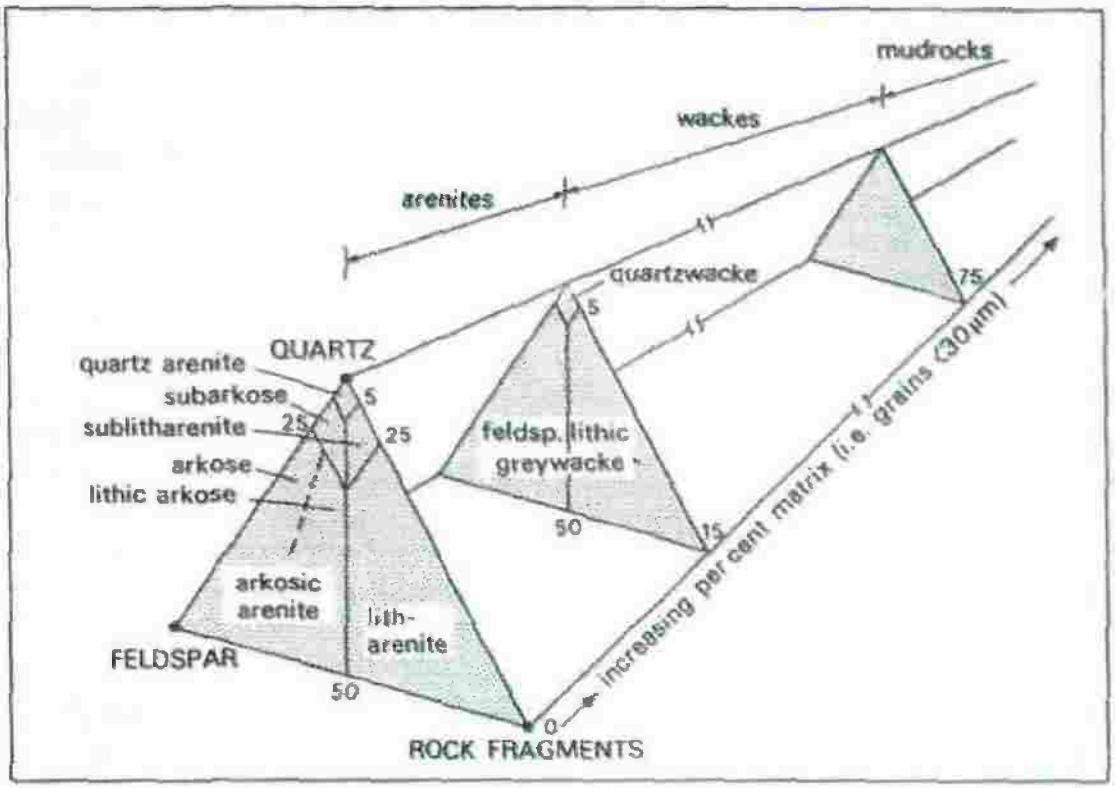

Fig. (3.7): Classification of sandstone (from Pettijohn et al., 1973).

3.4.1 Quartz arenite

This facies is applied as previously mentioned to rocks with 95% or more quartz grains, of these:

3.4.1.1 Calcareous quartz arenite, (Plate 3.2, Figs. A-C)

This lithofacies is recorded in the upper part of the Bahariya Formation in TSW-15 well. This lithofacies is composed mostly of quartz grains. They are well sorted, well packed, very fine to fine grains, medium grains are subordinate. Also, quartz grains are monocystalline, mainly subangular to subrounded. Few feldspars and oil smears are recorded. Visible porosity mainly secondary porosity, few fossil fragments.

3.4.1.2 Glaugonitic quartz arenite, (Plate 3.3, Figs. A-C)

This lithofacies is recorded in the upper part of the Bahariya Formation in TSW-15 and 21 wells. This lithofacies is composed mostly of quartz grains. Also, quartz grains are monocystalline, mainly subangular to subrounded.

3.4.1.3 Laminated sublithic quartz arenite, (Plate 3.4, Figs. A-C)

This lithofacies is recorded in Abu Roash `G` Member in TSW-21 well (Plate 3.4, Figs. A-B) and the upper part of the Bahariya Formation in TSW-7 well (Plate 3.4, Fig. C). This lithofacies is composed mostly of fine quartz grains. They are moderately sorted. Also, quartz grains are monocystalline, mainly subangular to subrounded. Lithoclasts are common and composed of fine well cemented quartz grains.

3.4.1.4 Subfeldspathic quartz arenite, (Plate 3.5, Fig. A)

This lithofacies is recorded in the lower part of the Bahariya Formation in BED1-11 well (Plate 3.5, Fig. A).This lithofacies is composed mostly of fine grained quartz grains. They are moderately sorted, well packed. Also, quartz grains are monocystalline, mainly subangular to subrounded. Secondary porosity filled by koalintes. Feldspars are subordinate, and carbonaceous materials are common.

3.4.1.5 Glauconitic subfeldspathic quartz arenite, (Plate 3.5, Fig. B)

This lithofacies is recorded in the lower part of the Bahariya Formation in BED1-11 well (Plate 3.5, Fig. B).

3.4.2 Quartz wacke:

This facies is applied as previously mentioned to rocks with 15% to 75% matrix, of these:

3.4.2.1 Massive quartz wacke, (Plate 3.6, Figs. A-B)

This lithofacies is recorded in the upper part of the Bahariya Formation in TSW-21 well (Plate 3.6, Fig. A). This lithofacies is composed mostly of very fine quartz grains. They are well sorted, well packed, very fine grains. Also, quartz grains are monocystalline, mainly subangular to subrounded. Also this lithofacies is recorded in Abu Roash `G` Member in TSW-21 well (Plate 3.6, Fig. B). This lithofacies is composed of ill sorted, well packed, very fine to fine grains, with subordinate medium grains. Also, quartz grains

are monocystalline, mainly angular to subangular floated in silty matrix frequent carbonaceous materials. Visible porosity mainly secondary porosity, few fossil fragments. The frequent mud matrix (Plate 3.6, Fig. A) and the bimodal occurrences of the quartz grains (Plate 3.6, Fig. B) are good indications for the estuary environment.

3.4.2.2 Laminated quartz wacke, (Plate 3.6, Fig. C)

This lithofacies is recorded in Abu Roash `G` Member in TSW-21 well. This lithofacies is composed of well sorted, well packed, very fine grains, with subordinate fine grains. Also, quartz grains are monocystalline, mainly subangular to subrounded floated in micritic matrix. The frequent laminations in this lithofacies and the fine grains are good indications for mild currents at the lower shore environments.

3.4.2.3 Glauconitic quartz wacke, (Plate 3.7, Figs. A-C)

This lithofacies is recorded in the upper part of the Bahariya Formation in TSW-15 well (Plate 3.7, Figs. A and C) and Abu Roash `G` Member in TSW-21 well (Plate 3.7, Fig. B). This lithofacies is composed mostly of medium grains quartz grains. They are well sorted, well packed, very fine to fine grains. Also, quartz grains are monocystalline, mainly subangular to subrounded floated in micritic matrix. The common glauconites are a good indication for the increase of marine environments and could be interpreted as transition zone.

Note: The description of the studied core samples and their thin sections have been compiled and displayed in tables in the appendices of the respective chapter.

Plate (3.1)

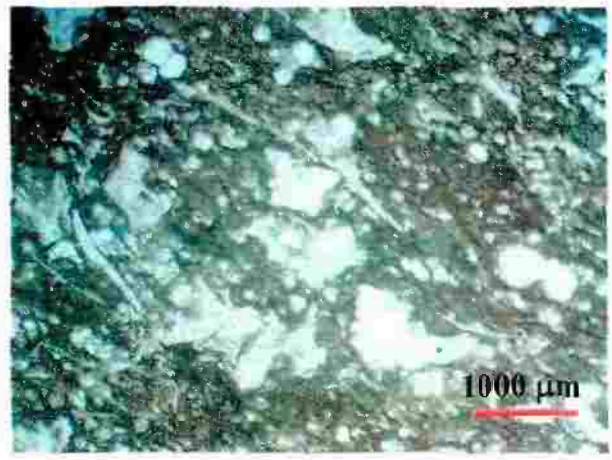

Fig. (A): Foraminiferal molluscan packstone. Photomicrograph showing foraminiferal packstone with foram tests and molluscan shells scattered in micritic matrix, low porosity (blue colour) could be seen on the periphery of the fossil grains, (Well: TSW-8, sample 58, Abu Roash `F` Member).

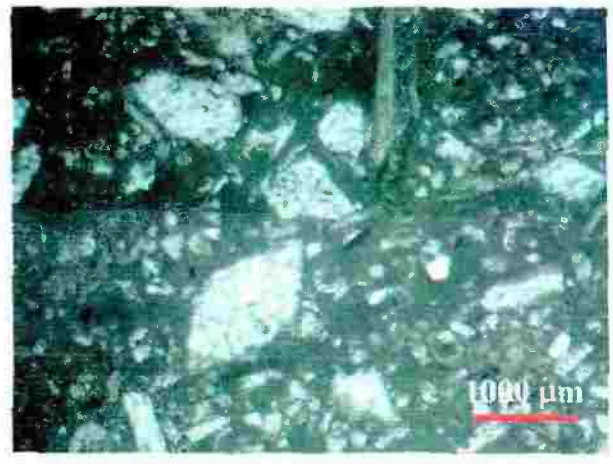

Fig. (B): Foraminiferal molluscan packstone. Photomicrograph showing foraminiferal packstone with foram tests and molluscan shells scattered in micritic matrix with completely microcrystalized fossils, (Well: TSW-21, sample 54, Abu Roash `G` Member).

Plate (3.2)

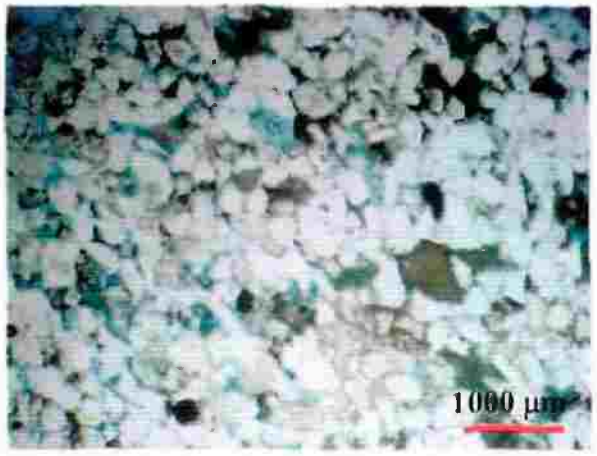

Fig. (A): Calcareous quartz arenite. Photomicrograph showing quartz arenite with fine to very fine quartz grains cemented with carbonate, intergranular porosity (blue colour) and few glauconitic grains,(Well: TSW-15, sample 7H1, U. Bahariya).

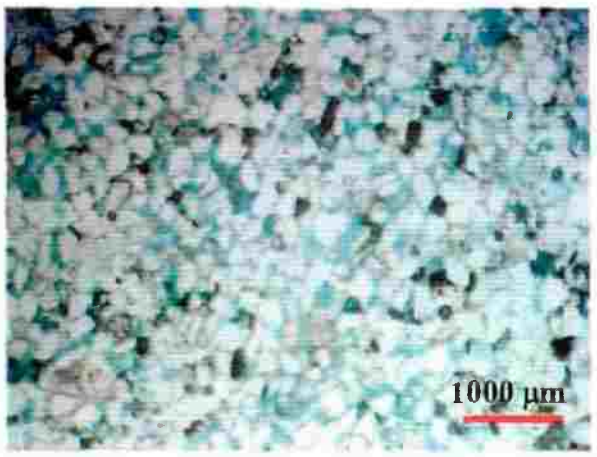

Fig. (B): Calcareous quartz arenite. Photomicrograph showing quartz arenite with fine to very fine quartz grains cemented with carbonate, intergranular porosity (blue colour) and few glauconite grains. Excellent porosity condition where the carbonate cement (aragonite) is thoroughly leached. (Well: TSW-15, sample 43H2, U. Bahariya).

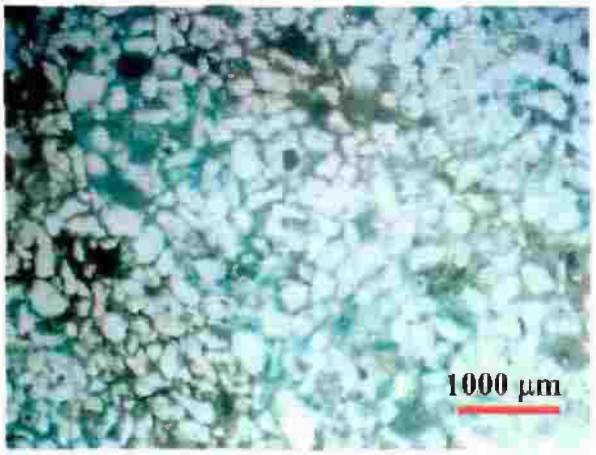

Fig. (C): Calcareous quartz arenite. Photomicrograph showing quartz arenite with fine to very fine quartz grains cemented with carbonate, intergranular porosity (blue colour) and few of glauconite. Quartz grains are open packed (bioturbated) in the middle part which in turn increase porosity, while the down left area is well packed. (Well: TSW-15, sample 11H1, U. Bahariya).

Plate (3.3)

Fig. (A): Glauconitic calcareous quartz arenite. Photomicrograph showing quartz arenite. It is glauconitic calcareous and ferruginous with secondary porosity due to diagenesis (blue colour). (Well: TSW-21, sample 45, U. Bahariya).

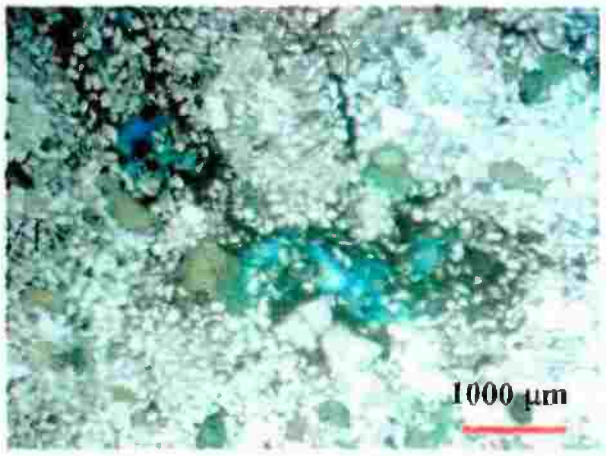

Fig. (B): Glauconitic calcareous quartz arenite. Photomicrograph showing quartz arenite. It is glauconitic calcareous and ferruginous with poor porosity (blue colour) due to high compaction and cementation. (Well: TSW-21, sample 45, U. Bahariya).

Fig. (C): Glauconitic quartz arenite. Photomicrograph showing quartz arenite. It is glauconitic, ferruginous, highly cemented, (Well: TSW-15, sample 6, U. Bahariya).

Plate (3.4)

Fig. (A): Fine laminated quartz arenite. Photomicrograph showing quartz arenite with laminated silt size to very fine quartz grains and ferruginous. The secondary porosity is due to leaching (blue colour), (Well: TSW-21, sample 9H1, Abu Roash `G` Member).

Fig. (B): Laminated quartz arenite. Photomicrograph showing quartz arenite with laminated very fine quartz grains, ferruginous, and intergranular porosity (blue colour) is recognized from coarser grains, (Well: TSW-21, sample 24H, Abu Roash `G` Member).

Fig. (C): Cross laminated quartz arenite. Photomicrograph showing quartz arenite, cross lamination, very fine quartz grains, ferruginous and intergranular porosity (blue colour), (Well: TSW-7, sample 2H2, U. Bahariya).

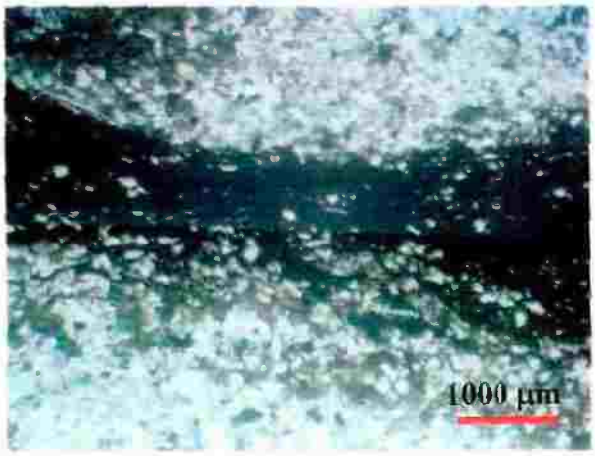

Plate (3.5)

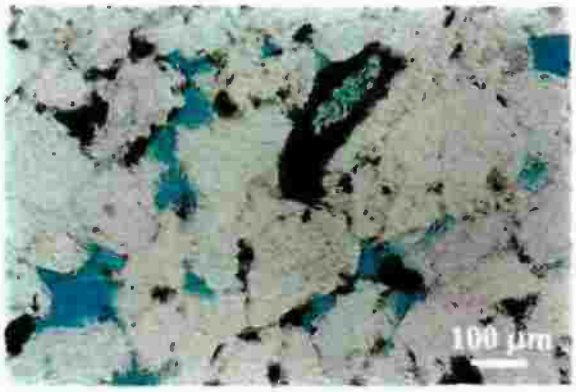

Fig. (A): Subfeldspathic quartz arenite. Photomicrograph showing medium grained, well sorted sandstone with pore lining and pore filling quartz overgrowths possessing euhedral crystal terminations around detrital quartz grains. Note the partly leached mica where the leached part is preferentially filled by kaolinite, (Well: BED1-11, sample 59, L. Bahariya).

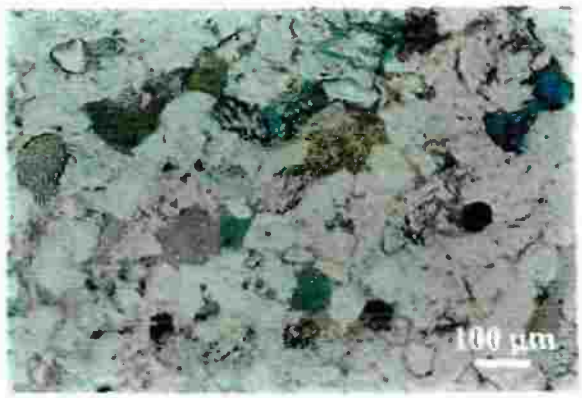

Fig. (B): Glauconitic subfeldspathic quartz arenite. Photomicrograph showing fine grained, moderately sorted sandstone composed of quartz grains, partly altered glauconite grains and minor leached feldspars. (Well: BED1-11, sample 63, L. Bahariya).

Plate (3.6)

Fig. (A): Massive quartz wacke. Photomicrograph showing quartz wacke with very fine quartz grains, well cemented and ferruginous with limited intergranular porosity (blue colour), (Well: TSW-21, sample 49, U. Bahariya).

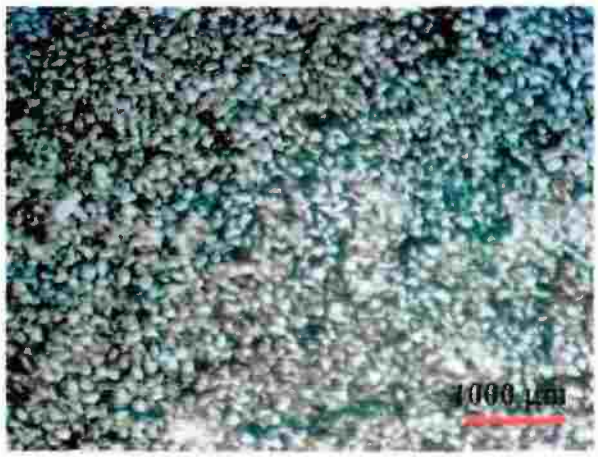

Fig. (B): Massive quartz wacke. Photomicrograph showing quartz wacke with very fine to medium quartz grains, ferruginous cement and low intergranular porosity (blue colour), (Well: TSW-21, sample 52, Abu Roash 'G').

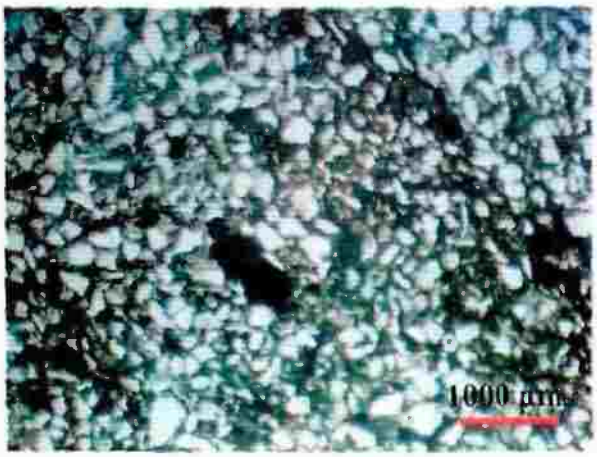

Fig. (C): Laminated quartz wacke. Photomicrograph showing quartz wacke with laminated very fine quartz grains, ferruginous and calcareous cement, few glauconite are also recognized, (Well: TSW-21, sample 16H1, Abu Roash 'G').

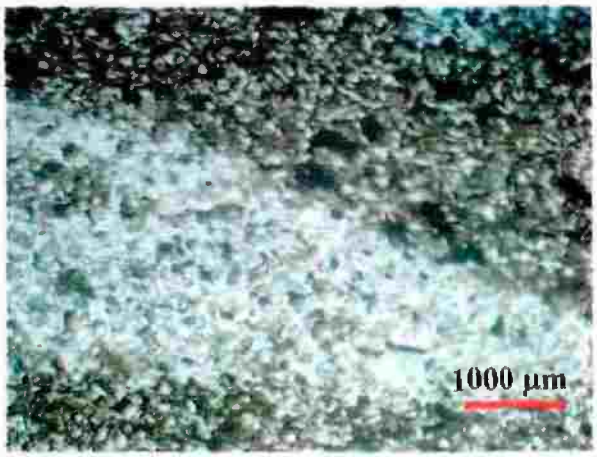

Plate (3.7)

Fig. (A): Glauconitic phosphatic quartz wacke. Photomicrograph showing quartz wacke with fine quartz grains, glauconite, phosphatic grains and intergranular porosity (blue colour), (Well: TSW-15, sample 3, U. Bahariya).

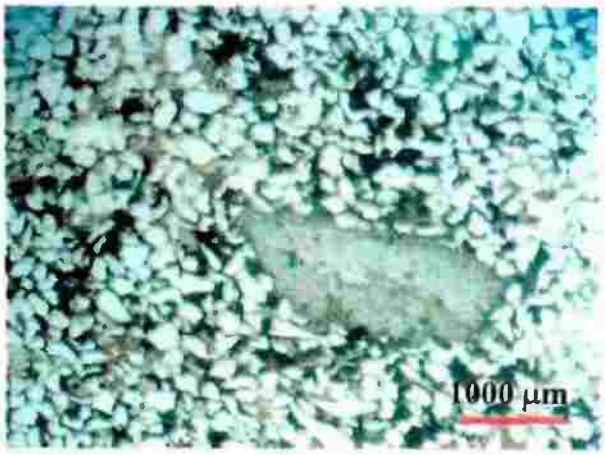

Fig. (B): Glauconitic quartz wacke. Photomicrograph showing quartz wacke with fine quartz grains, highly glauconitic, few phosphatic grains and intergranular porosity is observed (blue colour), (Well: TSW-21, sample 17, Abu Roash 'G').

Fig. (C): Glauconitic quartz wacke. Photomicrograph showing quartz wacke with very fine quartz grains and ferquent in fine glauconitic grains, (Well: TSW-15, sample 13H1, U. Bahariya).

3.5 Depositional Environments

The Upper Cretaceous facies (the Bahariya Formation and Abu Roash Members) are generally laid down under an estuary environment influenced by transgressive marine shelf facies. The following depositional environments have been recognized from the studied cores (Table 3.2) as follows:

1-Estuary: The zone or area of water in which freshwater and saltwater mingle and water is usually brackish due to daily mixing and layering of fresh and salt water. Sedimentation is affected by **(a)** changes in sea level; **(b)** paleotopography and **(c)** sediment supply. These sediments are mingled and organized by tidal currents. The sedimentary structures are mud drape ripples, rhytimic laminated heterolithic deposits, bidirectional cross stratifications, reactivation surfaces and tidal bundles (Howell & Flint, 2003). This environment is represented by heterolithic medium to fine sand and the lithology is wacke with clays. This environment is rare and has been found in the Bahariya Formation in wells BED1-11, TSW-21 and in Abu Roash 'G' in TSW-21 well (Plate: 3.6 A and B).

2-Shore face: this zone belongs to fluvial system with dominated wave action. The sediments are redistributed along the shore with wave ripples. Structures are planar and hummocky cross stratifications (Howell & Flint, 2003). The shore face shows gradation from shallow to deep water as follows:

A-Upper shore face: It is characterized by clean sands and well ordered cross stratification. This environment is represented by very clean cross bedded with very rare glauconite and the lithology is calcareous arenite. This environment has been found in the Bahariya Formation in wells BED1-11, TSW-7, TSW-15, TSW-21 and in Abu Roash 'G' in TSW-21 well (Plates: 3.2 C, 3.5 A and B).

B-Lower shore face: It is characterized by low angle cross laminations with intercalation of bioturbated siltstone and sandstone. This environment is represented by laminated fine sandstones with rare glauconite, rare rock fragments and the lithology is calcareous wacke. This environment has been found in the Bahariya Formation in wells BED1-11, TSW-7, TSW-15 and TSW-21, also in Abu Roash `G` in TSW-21 well (Plate: 3.6 C).

3-Offshore transition zone: It is characterized by hummocky cross stratifications sandstone, with intercalations of bioturbated siltstone and mudstone. This zone shows gross accumulations of glauconites. The prominent glauconite beds of this zone provide a visual key to recognizing transgressive-regressive cycles. This environment is represented by laminated sandstone, ripples with frequent glauconite, common rock fragments and the lithology is sublithic calcareous wacke. This environment has been found in the upper part of the Bahariya Formation in wells TSW-7 and TSW-15 (Plate: 3.7 A).

4-Offshore zone (a): It is characterized by massive mudstone, with intercalations of bioturbated siltstone and mudstone also some glauconites are also recorded. This environment is represented by laminated silt/mudstone, with common glauconite, rare fossils and the lithology is mudstone/siltstone. This environment has been found in the upper part of the Bahariya Formation in wells TSW-7 and TSW-15, also in Abu Roash `G` in TSW-21 well (Plate: 3.7 C).

5-Offshore zone (b): It is characterized by fossiliferous limestone, with micritic matrix. Also, some glauconites are recorded. This environment is represented by limestone, rare glauconites, common fossils and the lithology is carbonate. This environment has been found only in Abu Roash `F` in TSW-8 well and Abu Roash `G` in TSW-21 well (Plate: 3.1 A & B).

Table (3.2): Zones of the sedimentary shelf of the studied areas.

Characters	Estuary	Upper shore face	Lower shore face	Transition	Offshore (a)	Offshore (b)
Structure	heterolithic Medium/fine sand	very clean X-bedded	laminated fine sandstone	laminated sst ripples	laminated silt/mudstone	massive
Glauconite	-	very rare	rare	frequent	common	rare
Fossils	-	-	-	-	rare	common
Rock fragments	-	-	rare	common	-	-
Lithology	wacke with clays	calcareous arenite	calcareous wacke	sublithic calcareous wacke	mudstone/ siltstone	carbonate
Core plugs						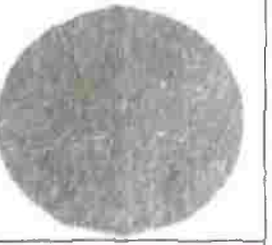
Thin sections of the plugs			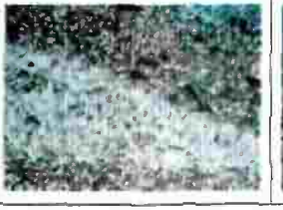			

Table (3.2), continued: Zones of the sedimentary shelf of the studied areas

Wells / Φ / K/ MHR/ pvc2	Estuary	Upper shore face	Lower shore face	Transition	Offshore (a)	Offshore (b)
TSW-7 samples	-	2, 19	42, 31	32, 10, 22, 40	1	-
TSW-8 samples	-	-	-	-	-	57, 58, 59, 36, 38, 50, 33, 41, 44, 12, 51
TSW-15 samples	-	28, 6, 55, 53, 18, 43, 11, 7	21	3	13	-
TSW-21 samples	52, 49	25, 9, 24, 45, 5	30, 16, 20, 37	-	17	54
BED1-11 samples	74	2,3,5,6,12-16,29, 30,41,44,46,48, 50,51,54,59,60, 62, 63, 65, 73	4, 7-9, 24, 25, 27, 28, 31, 39, 40, 47, 48, 52, 53, 56, 64, 74, 75, 76, 78, 79	-	-	-
Average Φ, %	12.5	16.6	10.9	15.3	14.4	15.9
Average K, md	0.06	46.3	5.36	1.05	0.09	0.018
Average MHR, μm	0.08	2.38	0.35	0.43	0.03	0.12
Average pvc2, % pv	69.1	25.7	54.6	52.1	74.6	40.4

SCANNING ELECTRON MICROSCOPE (SEM)

3.6 Methodology

Scanning electron microscope (SEM) model (Jeol 5300) was used in our search. A total of six (6) samples were examined for understanding the diagenesis processes. SEM is a powerful tool to illustrate the actual three-dimensional grain size relationships and details of the intergranular pore structure. It is a good tool to look down into the pores to identify the smallest mineral grains and the distribution of these minerals within the pores. Rock samples submitted for SEM analysis are supposed to be a fresh surface, uncontaminated by drilling fluids. To minimize contamination, oil-coated samples should be cleaned in a soxhlet extractor with solvents such as (1:4 chloroform–acetone) for one or two days. The cutting sample is attached to SEM specimen plug with epoxy or silpaste and dried overnight in a low temperature-drying oven. The sample is then coated with a conductive metal (i.e. gold). The coated SEM sample is placed in the sample chamber, in the electron optics column and evacuated to high vacuum. The SEM image is formed by an internally generated electron beam. This beam is created by heating a "hairpin" tungsten filament in the electron gun until the filament emits electrons. As the primary electron beam traverses the sample, the secondary electrons are emitted and collected by a secondary electron detector mounted in the SEM sample chamber and processed by the electronics console into the familiar SEM image. This image is displayed either on a TV screen and photographed with an attached camera. Figures (3.8) to (3.24) display the different SEM photos of the studied samples.

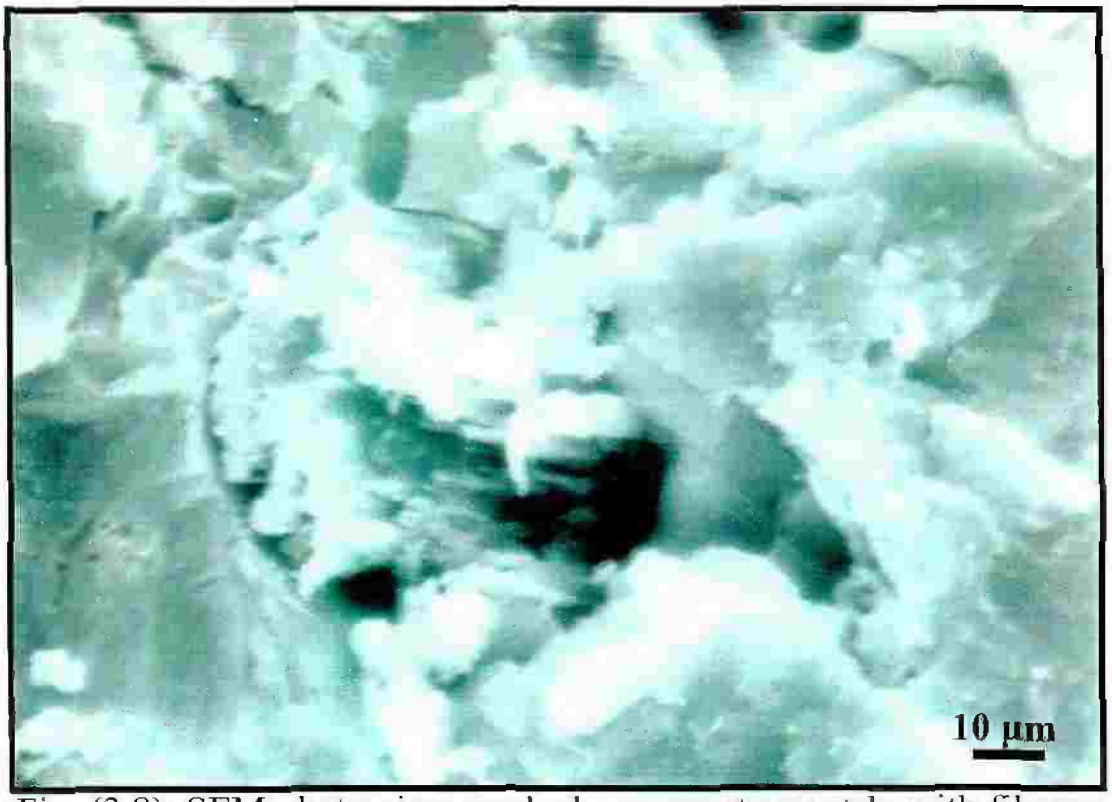

Fig. (3.8): SEM photomicrograph shows quartz crystals with fibrous texture in a surface pore, sample 40, ϕ=13.3%, k=0.08 md, U. Bahariya, TSW-7 well.

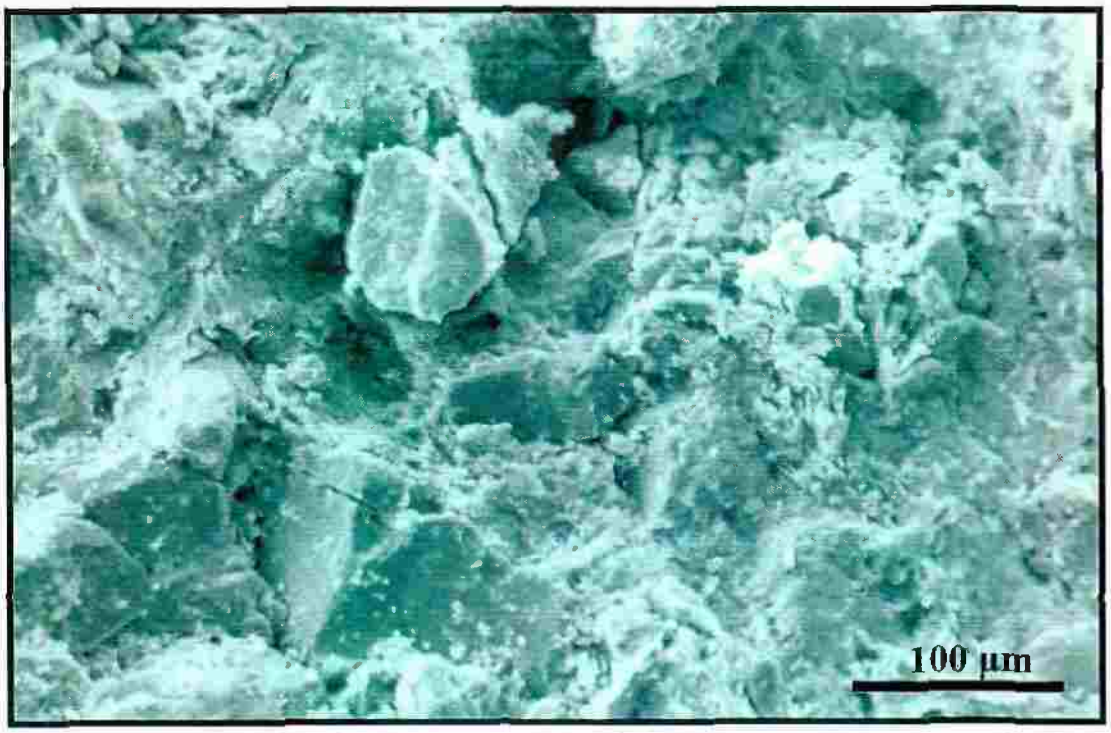

Fig. (3.9): SEM photomicrograph shows cementation by detrital materials, sample 11H1, ϕ=20.2%, k=14.5 md, U. Bahariya, TSW-15 well.

Fig. (3.10): SEM photomicrograph shows authigenic quartz overgrowths lining the intergranular pores, sample 11H1, ϕ=20.2%, k=14.5 md, U. Bahariya, TSW-15 well.

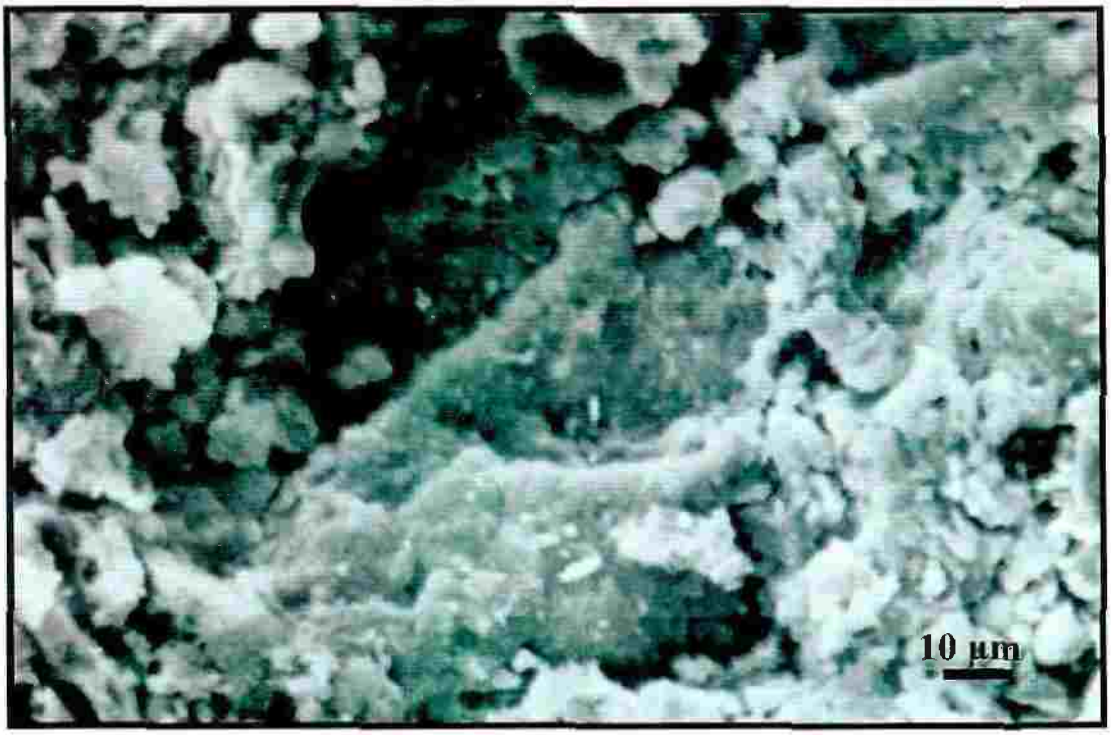

Fig. (3.11): SEM photomicrograph shows the intergranular porosity, sample 17, ϕ=21.8%, k=0.16 md, Abu Roash (G), TSW-21 well.

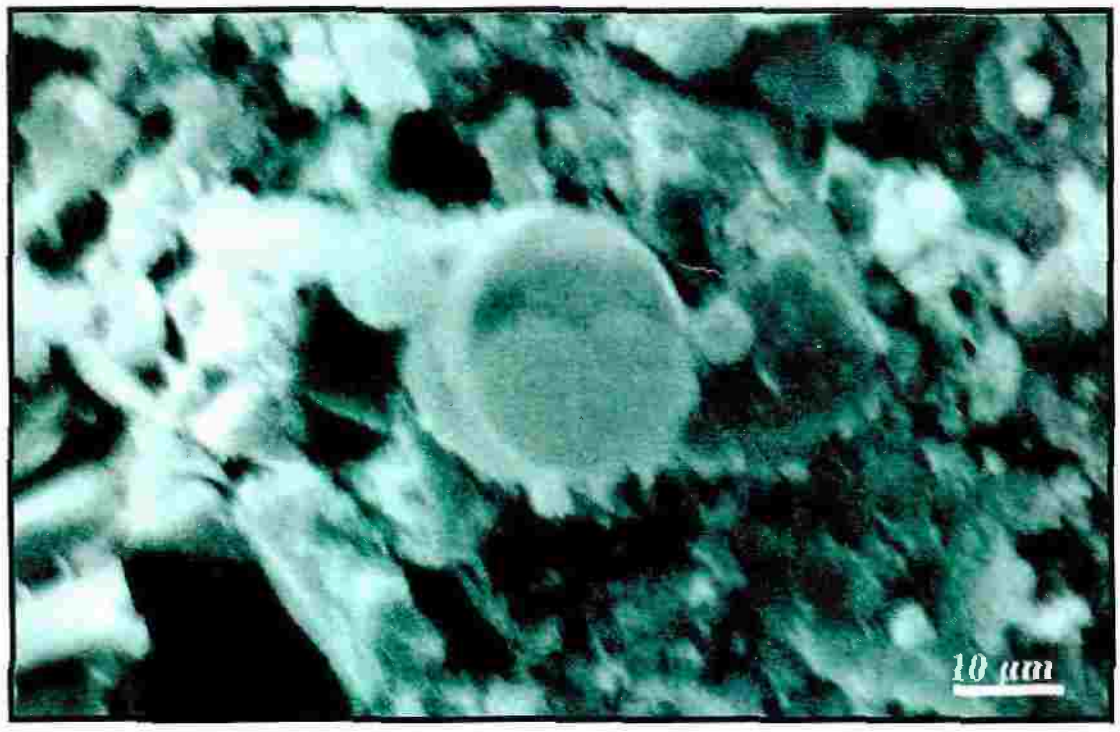

Fig. (3.12): SEM photomicrograph shows oval and rounded glauconite peloids, sample 17, ϕ=21.8%, k=0.16 md, Abu Roash (G), TSW-21 well.

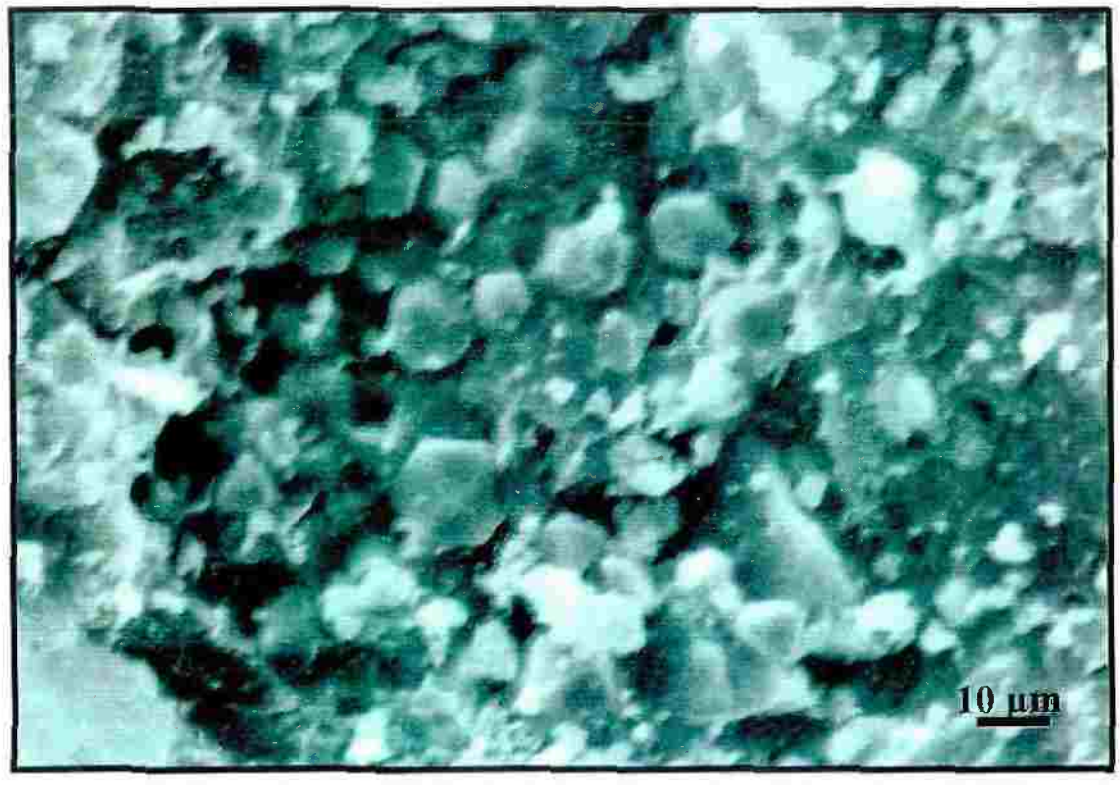

Fig. (3.13): SEM photomicrograph shows intergranular porosity and pyrite crystals, sample 49, ϕ=14.3%, k=0.043 md, U. Bahariya, TSW-21 well.

Fig. (3.14): SEM photomicrograph shows intergranular porosity and cementation by calcite, sample 49, ϕ=14.3%, k=0.043 md, U. Bahariya, TSW-21 well.

Fig. (3.15): SEM photomicrograph shows intergranular porosity and cementation by calcite, sample 49, ϕ=14.3%, k=0.043 md, U. Bahariya, TSW-21 well.

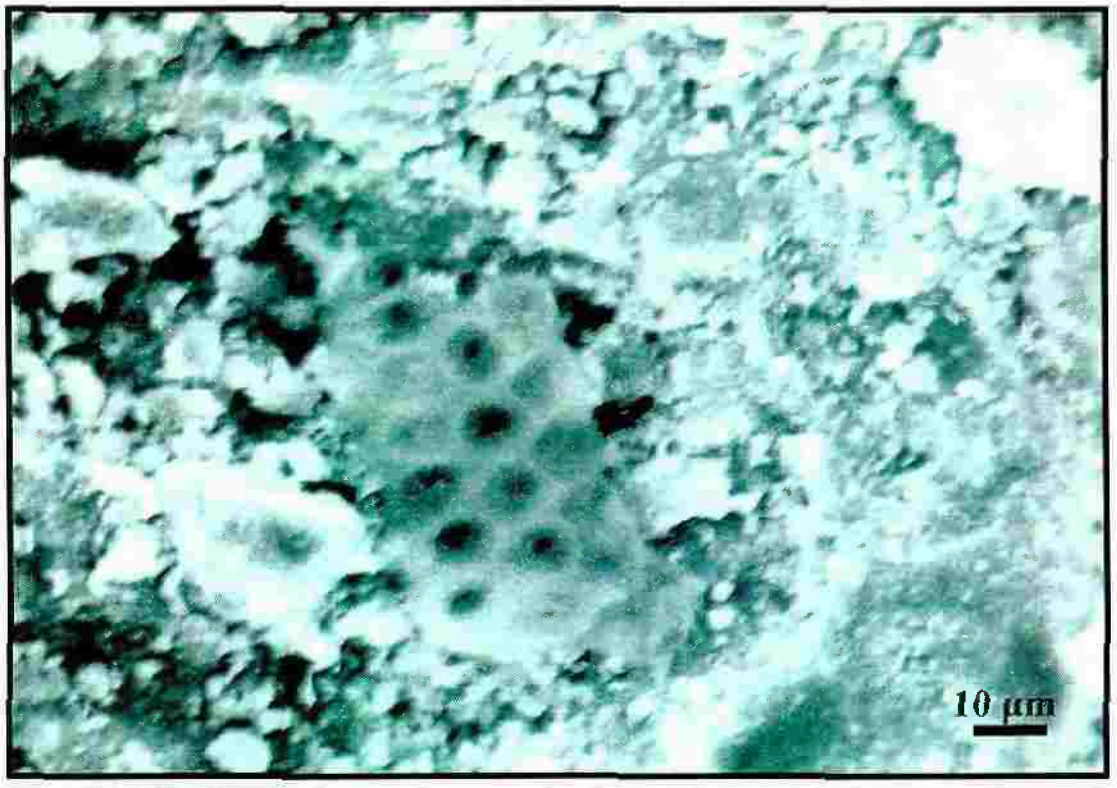

Fig. (3.16): SEM photomicrograph shows intergranular porosity and fossils disseminated in matrix, sample 45, ϕ=11.9%, k=0.20 md, U. Bahariya, TSW-21 well.

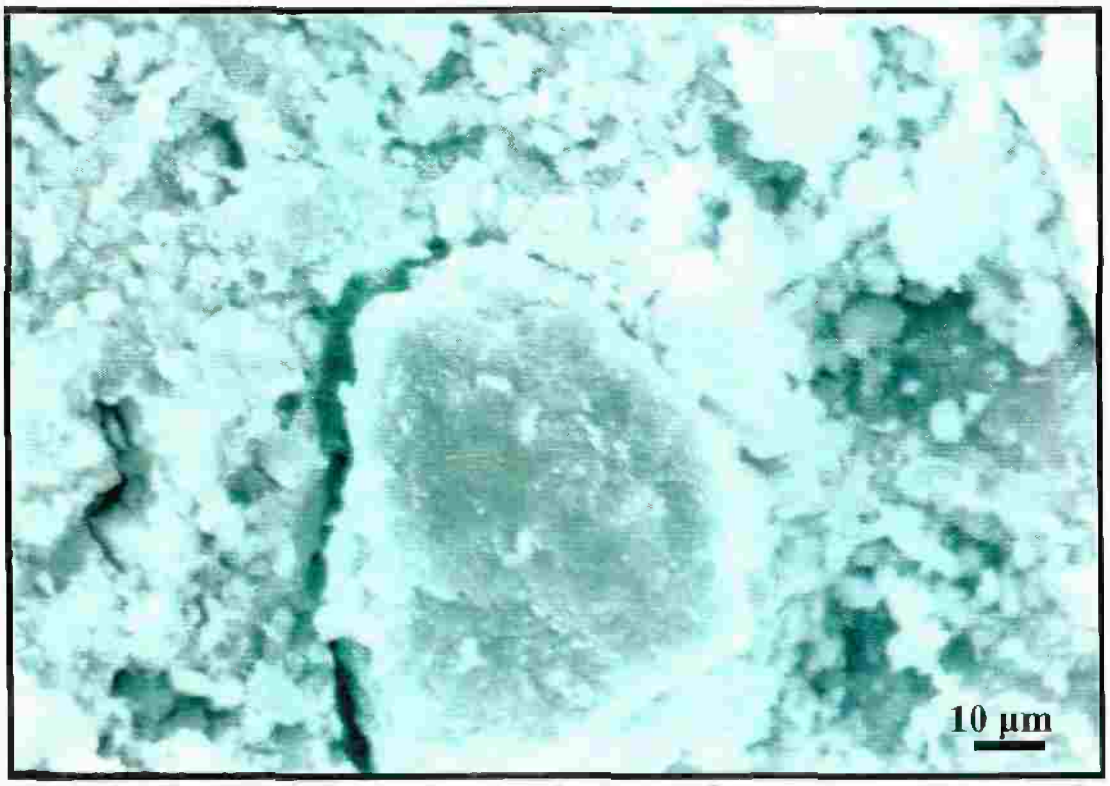

Fig. (3.17): SEM photomicrograph shows fracture porosity, sample 45, ϕ=11.9%, k=0.20 md, U. Bahariya, TSW-21 well.

Fig. (3.18): SEM photomicrograph shows cementation with carbonate which decreases the porosity, sample 45, ϕ=11.9%, k=0.20 md, U. Bahariya, TSW-21 well.

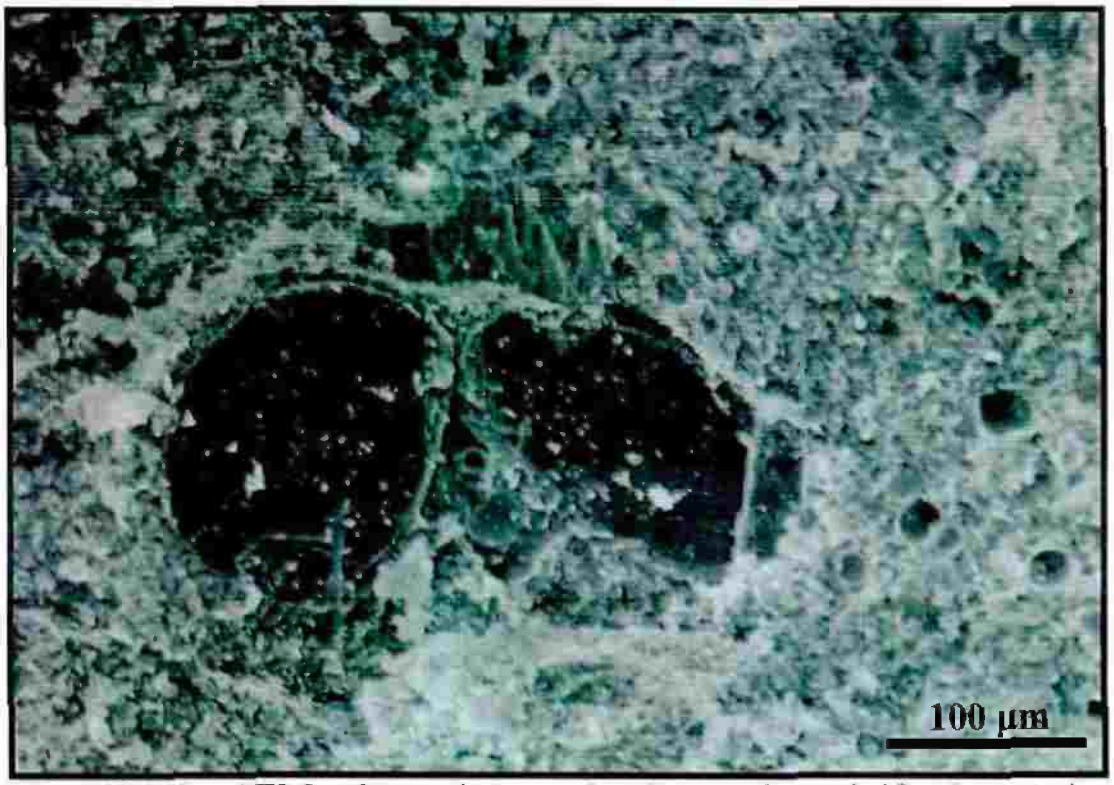

Fig. (3.19): SEM photomicrograph shows foraminiferal test in micrite cement, sample 58, ϕ=18.7%, k=0.045 md, Abu Roash (F), TSW-8 well.

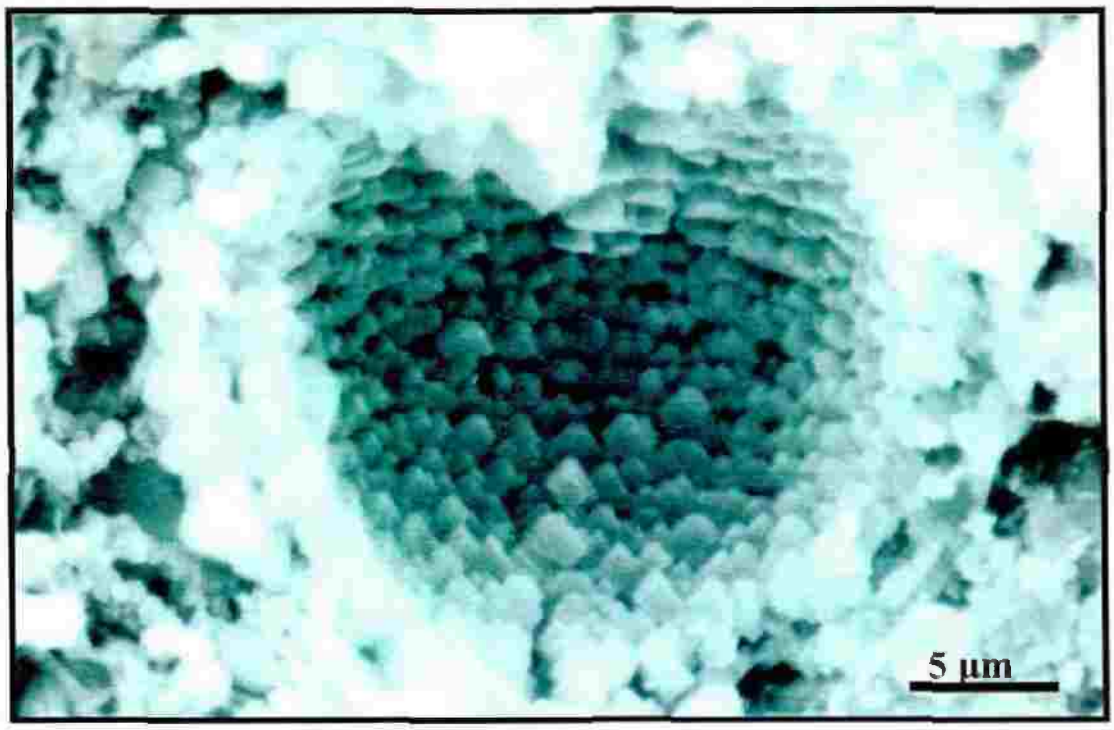

Fig. (3.20): SEM photomicrograph shows foraminiferal test filled with calcite crystals indicating diagenesis effects which decreases the porosity, sample 58, ϕ=18.7%, k=0.045 md, Abu Roash (F), TSW-8 well.

Fig. (3.21): SEM photomicrograph shows foraminiferal test filled with calcite crystals indicating diagenesis effects decreases the porosity, sample 58, ϕ=18.7%, k=0.045 md, Abu Roash (F), TSW-8 well.

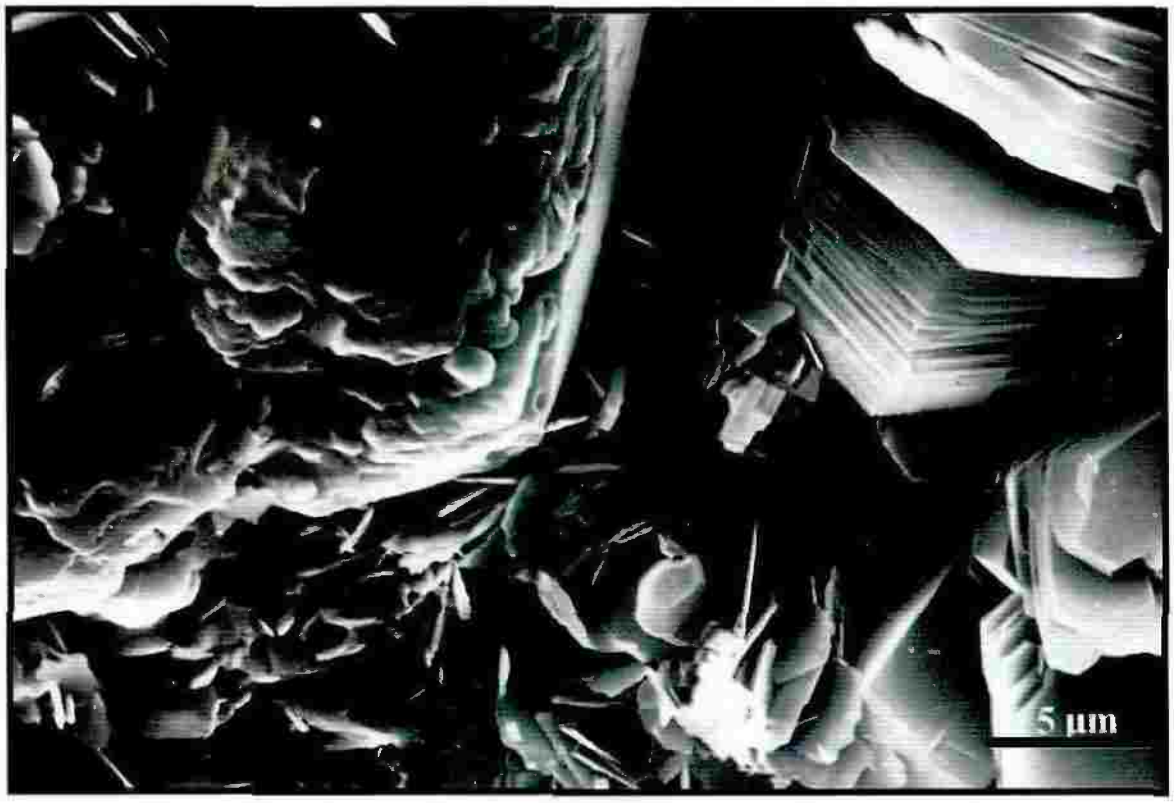

Fig. (3.22): SEM photomicrograph shows pore filling chlorite platelets, kaolinite booklets and dolomite. Note the corroded part of quartz grain with rough etched surface, sample 12, ϕ=14.9%, k=1.82 md, L. Bahariya, BED1-11 well.

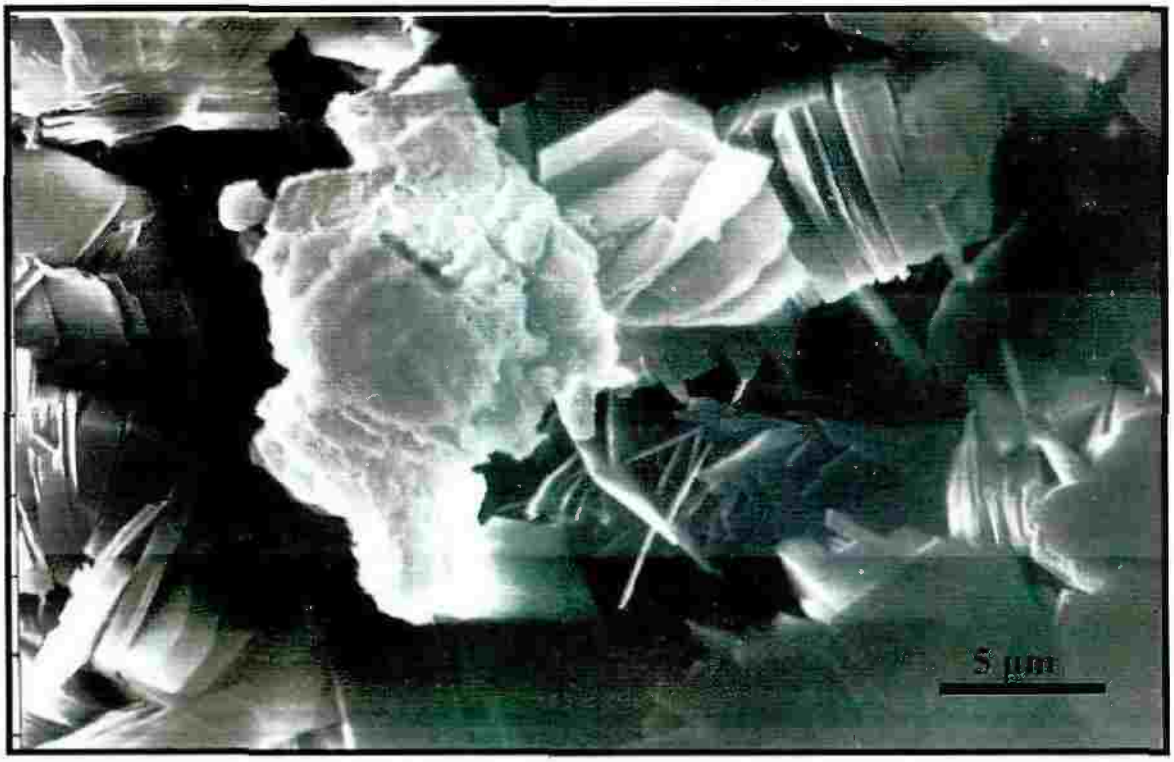

Fig. (3.23): SEM photomicrograph shows pore occluding kaolinite booklets in association with chlorite platelets, sample 63, ϕ=13.9%, k=17.3 md, L. Bahariya, BED1-11 well.

Fig. (3.24): SEM photomicrograph shows pore filling kaolinite booklets, quartz grains show well developed, euhedral quartz overgrowths around detrital grains. Note some of the kaolinite booklets embedded in the quartz overgrowths indicating contemporaneous nature of late stage quartz overgrowths and kaolinite precipitation, sample 12, ϕ=14.9%, k=1.82 md, L. Bahariya, BED1-11 well.

3.7 Results and discussion

The diagenentic features that have been recorded in SEM examined samples include pore-filling, authigenic well crystalline kaolinite booklets (kaolinite shows the classic platy, accordion-or book-like mineral form) and well crystalline calcite adjacent to well-developed authigenic quartz overgrowths. Glauconite is well illustrated in some samples. SEM examination reveals that the studied sandstones underwent considerable modification by different degrees during diagenesis. Early diagenesis involves mechanical compaction, grain coating and development of carbonate cement (Figs. 3.14, 3.15, 3.16 and 3.18). This was followed by the formation of quartz overgrowths (Figs. 3.10 and 3.24), framework grain dissolution, formation of chlorite (chlorite is

a common authigenic mineral lining the pores of sandstones). In some cases, the presence of authigenic chlorite on sand grains can inhibit the growth of pore-filling cements during diagenesis and preserve pore space for occupation by hydrocarbons), chlorite pore filling (the classic form is fiber pore bridge) plus kaolinite (Figs. 3.22, 3.23 and 3.24). Continued burial make the mixed clay layers to be more illite and associated with pyrite cementation (Fig. 3.13). A number of diagenetic processes have affected the reservoir quality of the studied samples as follows:

A-Processes that responsible for the reduction of primary porosity as:

-Carbonate cementation (Figs. 3.14, 3.15, 3.16 and 3.18), recognized in the upper part of the Bahariya Formation.

-Recrystallization of calcite inside the foram (Figs. 3.20 and 3.21), recognized in Abu Roash `F`.

-Quartz overgrowth (Figs. 3.10 and 3.24), recognized in the upper and the lower parts of the Bahariya Formation.

-Clay authigenesis (Figs. 3.22, 3.23 and 3.24), recognized in the lower part of the Bahariya Formation.

B-Processes that responsible for the porosity enhancement:

-Dissolution of carbonate cement (Fig. 3.19), recognized in Abu Roash `F`.

-Framework grain dissolution mainly glauconite (Fig. 3.12), recognized in Abu Roash `G`.

-Fracturing (Fig. 3.17), recognized in the upper part of the Bahariya Formation.